Temperature dependence of surface morphology and deuterium retention in polycrystalline ITER-grade tungsten exposed to low-energy, high-flux D plasma

V.Kh. Alimov[1,2,*], B. Tyburska-Püschel[3], S. Lindig[3], Y. Hatano[1], M. Balden[3], J. Roth[3], K. Isobe[2], M. Matsuyama[1], T. Yamanishi[2]

[1]*Hydrogen Isotope Research Center, University of Toyama, Toyama 930-8555, Japan*

[2]*Tritium Technology Group, Japan Atomic Energy Agency, Tokai, Ibaraki 319-1195, Japan*

[2]*Max-Planck-Institut für Plasmaphysik, EURATOM Association, D-85748 Garching, Germany*

Abstract

Surface topography and deuterium retention in polycrystalline ITER-grade tungsten have been examined after exposure to a low-energy (38 eV/D), high-flux (10^{22} D/m^{2}s) deuterium plasma with ion fluences of 10^{26} and 10^{27} D/m^2 at various temperatures. The methods used were scanning electron microscopy equipped with focused ion beam, thermal desorption spectroscopy, and the D(^{3}He,p)^{4}He nuclear reaction at ^{3}He energies varied from 0.69 to 4.0 MeV. During exposure to the D plasma at temperatures in the range from 320 to 815 K, small blisters of size in the range from 0.2 to 5 μm, depending on the exposure temperature and ion fluence, are formed on the W surface. At an ion fluence of 10^{27} D/m^2, the deuterium retention increases with the exposure temperature, reaching its maximum value of about 10^{22} D/m^2 at 500 K, and then decreases below 10^{19} D/m^2 at 800 K.

Keywords: Blistering; Deuterium; Deuterium retention; High ion flux; Tungsten

[*]Corresponding author. Tel.:+81 76 445 6934; fax: +81 76 445 6931.

E-mail address: vkahome@mail.ru (V.Kh. Alimov).

1. Introduction

Due to its favorable physical properties, like low erosion yield and high melting temperature, tungsten (W) is foreseen as one of plasma-facing materials in fusion reactors, such as ITER [1] and DEMO [2]. As a plasma-facing material, W will be subjected to intense fluxes of low-energy deuterium (D) and tritium particles. Available data ([3] and references therein) show that hydrogen isotope retention in W materials exposed to low-energy, high-flux hydrogen plasmas differs from that for low-energy ion implantation. Quite often the hydrogen retention is accompanied by formation of blister-like surface structures ([3] and references therein, [4, 5, 6, 7, 8, 9]. However, the temperature dependence of blistering and hydrogen isotope retention after exposure to low-energy (38 eV/D), high flux (10^{22} D/m^{2}s) deuterium plasma at high ion fluences ($\geq 10^{26}$ ions/m^2) was studied systematically for recrystallized W only [6-9]. The main objective of the present work was to extend the range of examined W materials to polycrystalline ITER-grade W. The ITER-grade W is deformed (rolled, swaged and/or forged) followed by appropriate heat-treatments to obtain better mechanical properties, e.g., strength and toughness, following the sintering process [10, 11].

2. Experimental

In these experiments, ITER-grade W delivered from A.L.M.T. Corp. (Japan) was used. The W material has a purity of 99.99 wt.% with main impurities being Mo, Fe, C and O. Square-shaped samples, 10×10 mm^2 in size and 2 mm in thickness, were so prepared by the manufacturer that the irradiated surfaces were perpendicular to deformation axis (i.e., to the heat transfer direction), which corresponds to the ITER specification[10, 11]. The samples were mechanically polished, cleaned in acetone ultrasonic bath, and then annealed in vacuum at 1473 K for 30 min for stress relief.

The surface topography and cross-sections of the samples were examined by scanning electron microscopy (SEM) (KEYENCE, Real Surface View Microscope VE-9800 and FEI, Helios NanoLab 600). According to cross-section images obtained by SEM combined with focused ion beam cross-sectioning (FIB), the microstructure of the Japanese ITER-grade W consists of anisotropically elongated grains along the deformation axis (Fig. 1). The grain size is 1-3 μm in section and up to 5 μm in length. Individual elongated cracks observed between grains (Fig. 1) are due to the deformation treatment.

The linear plasma generator (JAEA, Tokai) used for delivering a plasma beam comparable to the edge plasma at ITER divertor is described elsewhere [12]. To generate D plasma, D_2 gas was filled in the plasma generation section to a pressure of about 1 Pa. As a consequence, the plasma beam contained species of D_2^+ (over 80%) and D^+ (less than 20%) [12]. A bias voltage of -80 V was applied to the W sample, resulting in incident energy of 76 eV for D_2^+ (38 eV/D), taking into account the plasma potential of about -4 V as measured by a Langmuir probe. The incident deuterium ion flux was fixed at 10^{22} D/m^{2}s, and the samples were exposed to ion fluences of 10^{26} and 10^{27} D/m^2. The sample was passively heated by the plasma itself and the exposure temperature was set by the thermal contact between the specimen and the cooled holder. The temperature was monitored using a type K thermocouple tightly pressed to the rear of the sample.

The deuterium profiles in the plasma-exposed W samples were determined by nuclear reaction analysis (NRA) at IPP, Garching. The D(^{3}He,p)^{4}He reaction was utilized, and both the α particles and protons were analyzed. To determine the D concentration at larger depths, an analyzing beam of ^{3}He ions with energies varied from 0.69 to 4.0 MeV was used. The proton yields measured at different ^{3}He ion energies allow measuring the D depth profile in W at depths of up to 7 μm [13].

Total deuterium retention in the W samples was monitored ex-situ using thermal desorption spectrometry (TDS). An infrared heater was used to heat the samples at a ramp rate of 0.5 K/s and the sample temperature was raised to 1300 K. HD, and D_2 molecules released during TDS run were monitored by a quadrupole mass spectrometer (QMS). To calculate the relative contribution of the recorded HD and D_2 masses to the total release of deuterium, the partial currents of the QMS were normalized as described in Ref. [14]. A standard D_2 leak with an inaccuracy better than 10% was employed to calibrate the QMS after each TDS analysis.

3. Results

3.1. Surface topography

After exposure to an ion fluence $\Phi = 10^{26}$ D/m^2 at a temperature T_{exp} = 335 K, only sparse blisters of sizes 0.5-2 μm are observed on the surface (Fig. 2a). At T_{exp} = 410-490 K, the blisters increase slightly in size, and the maximum blister size reaches 4 μm (Fig. 2c). As the exposure temperature increases further, blister sizes decrease and are 0.5-2 μm at T_{exp} = 610-725 K (Fig. 2e).

The increase in a fluence to 10^{27} D/m^2 might lead to an insignificant increase in blister sizes. The maximum size of blisters, around 5 μm, seems to be observed at T_{exp} = 420-500 K (Fig. 2d). The blisters are arranged inhomogeneously in groups on the surface and blister sizes differ between the groups.

3.2. Thermal desorption spectra

The thermal desorption spectrum of deuterium obtained after loading with a fluence Φ = 10^{26} D/m^2 at exposure temperature T_{exp} = 335 K consists of a main peak centred at a temperature $T_{peak} \cong$ 510 K with a small peak appearing as a shoulder at $T_{peak} \cong$ 630-650 K (Fig. 3a). However, after D plasma exposure to $\Phi = 10^{27}$ D/m^2 at T_{exp} = 320 K, the ~650 K peak becomes dominating (Fig. 3b).

For $\Phi = 10^{26}$ D/m^2, as the exposure temperature increases, the main TDS peak is shifted towards higher temperatures (Fig. 3a). On the other hand, the tenfold increase in an ion fluence at the same exposure temperature results in a shift of TDS peaks to higher temperature also (compare panels (a) and (b) in Fig. 3). However, after exposure to $\Phi = 10^{27}$ D/m^2 at temperatures in the range from 565 to 650 K, the main TDS peaks are positioned practically at the same temperature $T_{peak} \cong$ 1070 K.

It should be noted that after plasma exposure at temperatures and fluences when small blisters are formed on the ITER-grade W surface, the TDS spectra do not demonstrate intensive bursting release, as happens with relatively large blisters (5-50 μm in size) formed on the surface of recrystallized W [6, 15] and hot-rolled W [16, 17] exposed to D plasmas.

3.3. Depth profiles

In the ITER-grade W exposed to the D plasma near room temperature (T_{exp} = 335 K) to an ion fluence $\Phi = 10^{26}$ D/m^2, deuterium depth profile is characterized by a sharp near-surface concentration maximum of about 2 at.%, and, at depths of 1 μm, by a concentration of (5-8)×10^{-2} at.% decreasing into the bulk by one order of magnitude between 1.5 and 7 μm (Fig. 4a). As the exposure temperature increases up to 490 K, the D concentration in the near-surface decreases, whereas the concentration at depths of 1-7 μm is nearly constant at about 0.2-0.3 at.%. Further increase of the exposure temperature leads to a decrease of the D concentration (Fig. 4a). Note that concentration minima at depths around 1 μm (Fig. 4) could be explained by thermal migration and release of D atoms for a time after termination of the exposure.

As the ion fluence increases up to 10^{27} D/m^2 near room temperature (T_{exp} = 320 K), the D concentration at depths of 1-7 μm increases but still decreasing with depth. At T_{exp} = 420-500 K, the D profiles demonstrate the concentration of 0.3-0.5 at.% with no decrease into the bulk (Fig. 4b). It is pertinent to note that the same D concentration is observed for $\Phi = 10^{26}$ D/m^2 at T_{exp} = 490 K (Fig. 4a). A peculiarity of D accumulation at temperatures of 600-700 K is that the D concentration at analyzable depths increases practically linearly with the ion fluence (Fig. 4, compare panels (a) and (b)).

It should be noted that the ITER-grade W contains intrinsic intergranular cracks (Fig. 1), and these defects could provide trapping of hydrogen isotopes in the bulk of the ITER-grade W at elevated temperatures.

3.4. Total retention

In the ITER-grade W exposed to the D plasma at $\Phi = 10^{26}$ D/m^2, total deuterium retention determined by TDS is (3-4)×10^{20} D/m^2 at T_{exp} = 320 K and, as exposure temperature increases, rises to its maximum of about 3×10^{21} D/m^2 at T_{exp} = 490 K and then decreases down to about 5×10^{19} D/m^2 at T_{exp} = 725 K (Fig. 5). Increasing the fluence to 10^{27} D/m^2 results in an increase of the total D retention by a factor of about 3 over the exposure temperature range between 320 K to 600 K (Fig. 5).

From the comparison of the TDS and NRA data (Fig. 5) it is clear that at $\Phi = 10^{26}$ D/m^2 and irradiation temperatures up to 500 K, 50-60% of retained deuterium is localized in the sub-surface layer up to 7 μm. This fraction drops to about 10% for higher temperatures beyond the maximum in the D retention. However, at $\Phi = 10^{27}$ D/m^2 the fraction of deuterium retained at depths up to 7 μm already decreases from about 60% to less than 20% with increasing exposure temperature before the maximum in the total retention is reached. In the temperature range from 500 to 700 K, this fraction increases from 10% back to 50% (Fig. 5).

4. Discussion

In the Japanese ITER-grade W exposed to the low-energy, high-flux D plasma, the depths of D accumulation (several micrometers) are much larger than the deuterium implantation range (several nanometers), and D concentration at depths of several micrometers reaches relatively high values of 0.01-0.5 at.%, depending on irradiation temperature (Fig. 4). Note that in

recrystallized W exposed to the same D plasma at temperatures of 480-540 K the D concentration reaches 1-2 at.%. [9, 15].

The mechanism of plastic deformation due to deuterium supersaturation [18] must be considered for modification of the subsurface structure and formation of trapping sites for deuterium [4, 7, 19]. During exposure to low-energy, high-flux D plasma, the D concentration in the implantation zone greatly exceeds the solubility limit and stresses the matrix lattice until plastic deformation occurs to alleviate these tensions [18]. This deformation is assumed to be responsible for the generation of vacancies, vacancy complexes and microscopic cavities, and for the concurrent accumulation of diffusing deuterium. Diffusing D atoms recombine on the cavity surfaces, increasing thus the D_2 gas pressure inside these cavities. The stress from supersaturation of D in the lattice is additionally increased by the high gas pressure inside the cavities.

As illustrated for the example of recrystallized W [7], at exposure temperatures above the brittle-to-ductile transition temperature (BDTT) (370-470 K depending on the crystal-lattice orientation [20]) the dislocation mobility is increased and the stress can be relaxed by dislocations moving along lattice planes through the whole crystallite leading to formation of large cavities (100-1000 μm^3) at the grain boundaries at depths of several tens of micrometers [7]. This corresponds to the material migration above the surface, i.e., the blister-like surface topography. Near room temperature, i.e. below BDTT, the stress relaxation results in brittle crack formation inside the grains [7, 21].

However, the temperature dependence of the surface morphology modification for the ITER-grade W exposed to the low-energy, high-flux D plasma differs from that for the recrystallized W (Fig. 6). Blisters formed on the ITER-grade W surface are significantly less in size than those on the recrystallized W. Using a field emission SEM combined with a focused ion beam (FIB) for examination of the sub-surface morphology of the ITER-grade W exposed to the D plasma at temperatures in the range from 320 to 600 K, Lindig et al. [21] have observed only blister-associated cracks elongated in parallel to the surface, without formation of large cavities and extrusions along slip systems like in the recrystallized W, with the exception of solitary cavities formed inside large grains. The blister-associated cracks in the ITER-grade W are localized at depths of several hundreds of nanometers in the near-surface layer strongly distorted by mechanical polishing.

Obviously, the mechanically damaged layer contains high density of dislocation type defects even after post-polishing annealing at 1473 K, and these defects promote formation of the stress-induced cracks under D plasma exposure. As gas pressure inside the cracks increases, cooperative fracture between the cracks suddenly becomes an easy way of relieving their overpressure, thus initiating elongated cracks and lifting the surface off into dome-shaped blisters.

The damaged layer with the cracks may serve as a damper to dissipate the compressive stresses induced by the local deuterium supersaturation and prevent formation of plasma-induced cracks and cavities beneath the mechanically damaged near-surface layer, i.e., in the bulk on the ITER-grade W.

It is pertinent to remind that intrinsic intergranular cracks (Fig. 1) are a feature of the bulk structure of the ITER-grade W. These cracks may contribute to the trapping of deuterium in the bulk of the W material both in the molecular form inside the cracks and as D atoms chemisorbed at the walls of the cracks. Other type of defects like vacancies, grain boundaries and dislocations can also serve as D trapping sites.

After exposure to the same low-energy, high-flux D plasma to a fluence of 10^{26} D/m^2 at temperatures below 500 K, the D retention in the ITER-grade W is higher than that for recrystallized W[a)] [9, 15, 21] (Fig. 7). This finding can be explained by relatively high concentration of the intrinsic defects in the bulk of the mechanically deformed ITER-grade W. However, at exposure temperatures between 500 and 600 K, large plasma-induced distortions, intragranular cracks and large cavities at the grain boundaries are formed in the recrystallized W [7], whereas, as it was mentioned above, the bulk structure of the ITER-grade W remains unaltered. As a consequence, at T_{exp} = 500-600 K the recrystallized W demonstrates higher D retention than the ITER-grade W (Fig. 7). At exposure temperatures above 600 K, a difference in the D retention for these W materials becomes insignificant.

For highest ion fluence of 10^{27} D/m^2, the temperature dependences of the D retention for both W materials are practically the same (Fig. 7). However, a comparison of deuterium depth profiles in these W material after exposure to the highest D ion fluence (Fig. 4 and [9, 15]) shows that the D retention within the sub-surface layer (up to 7 μm in thickness) in the ITER-

[a)] The recrystallized W samples were prepared by annealing of the mechanically polished ITER-grade W samples in a dry hydrogen atmosphere at 2073 K for 1 h. The recrystallized W is characterized by large grains of size 20-200 μm and lack of intergranular cracks [7].

grade W is lower by a factor of about two than that in the recrystallized W. Thus, it is believed that in the ITER-grade W deuterium retained deeper into the bulk than in the recrystallized W. This is inline with higher defects density in the bulk of the ITER-grade W.

5. Summary

Insignificant temperature dependence of surface morphology is found for mechanically polished ITER-grade W exposed to low-energy (38 eV/D), high-flux (10^{22} D/m^{2}s) D plasma at ion fluences of 10^{26} and 10^{27} D/m^2. During D plasma exposure at temperatures in the range from 320 to 815 K, only small blisters of size in the range from 0.2 to 5 μm are formed on the W surface. Blister-associated cracks elongated in parallel to the surface are localized at depths of several hundreds of nanometers in the near-surface layer strongly distorted by mechanical polishing.

Intrinsic intergranular cracks in the bulk of the ITER-grade W provide deuterium accumulation up to relatively high concentration. At ion fluences of 10^{26} and near room temperature, the D concentration is characterized by a sharp near-surface concentration maximum of about 2 at.%, and, at depths of 1 μm, by a concentration of $(5\text{-}8)\times10^{-2}$ at.% decreasing into the bulk. As the ion fluence increases up to 10^{27} D/m^2, the D concentration in the bulk increases. For both ion fluences at exposure temperatures of 420-500 K, the D concentration at depths of 1-7 μm reaches 0.3-0.5 at.%. An increase of the exposure temperature leads to a decrease of the D concentration. However, a peculiarity of D accumulation at temperatures of 600-700 K is that the D concentration at analyzable depths of 7 μm increases practically linearly with the ion fluence, whereas the total retention increases only by a factor less than three.

Stress-induced plastic deformation caused by deuterium supersaturation is suggested as mechanisms for formation of microscopic cracks in the near-surface layer damaged by mechanical polishing. Diffusing D atoms recombine on the crack surfaces, increasing thus the gas pressure inside these cracks and lifting the surface off into dome-shaped blisters.

The near-surface mechanically damaged layer with the cracks is speculated to may serve as a damper to dissipate the compressive stresses induced by the local deuterium supersaturation and prevent formation of plasma-induced cracks and cavities in the bulk on the ITER-grade W.

Figure capture

Figure 1. SEM/FIB cross section image of polycrystalline ITER-grade W (tilted by 38°).

Figure 2. SEM images of polycrystalline ITER-grade W exposed to low-energy (38 eV/D), high-flux (10^{22} D/m^2 s) D plasma with ion fluences, Φ, of 10^{26} D/m^2 (a, c, e – left part of the figure) and 10^{27} D/m^2 (b, d, f – right part of the figure) at indicated temperatures. The scale bar given in panel (f) is valid for all images. The surfaces were tilted at an angle of 45° to the electron beam.

Figure 3. Thermal desorption spectra of deuterium released from polycrystalline ITER-grade W exposed to low-energy (38 eV/D), high-flux (10^{22} D/m^2 s) D plasma with ion fluences of 10^{26} (a) and 10^{27} D/m^2 (b) at various temperatures. The TDS heating rate was 0.5 K/s. Note that the deuterium release rate scales in panels (a) and (b) differ by a factor of 2.5.

Figure 4. Depth profiles of deuterium retained in polycrystalline ITER-grade W exposed to low-energy (38 eV/D), high-flux (10^{22} D/m^2 s) D plasma with ion fluences of 10^{26} (a) and 10^{27} D/m^2 (b) at various temperatures.

Figure 5. Deuterium retention in polycrystalline ITER-grade W exposed to low-energy (38 eV/D), high-flux (10^{22} D/m^2 s) D plasma with ion fluences of 10^{26} and 10^{27} D/m^2, as a function of the exposure temperature. The total deuterium retention was determined by thermal desorption spectrometry (TDS) (filled symbols), whereas the D retention up to a depth of 7 μm was measured by nuclear reaction analysis (NRA) (open symbols).

Figure 6. SEM images of recrystallized W (rc-W) (a, c, e – left part of the figure) [9, 15] and polycrystalline ITER-grade W (ITER-W) (b, d, f – right part of the figure) exposed to low-energy (38 eV/D), high-flux (10^{22} D/m^2 s) D plasma with an ion fluence of 10^{27} D/m^2 at indicated temperatures. The scale bar given in panel (e) is valid for all images. The surfaces were tilted at an angle of 45° to the electron beam.

Figure 7. Total deuterium retention in recrystallized W [9, 15] and polycrystalline ITER-grade W exposed to low-energy (38 eV/D), high flux (10^{22} D/m^2 s) D plasma with ion fluences of 10^{26} and 10^{27} D/m^2, as a function of the exposure temperature. The total deuterium retention was determined by thermal desorption spectrometry.

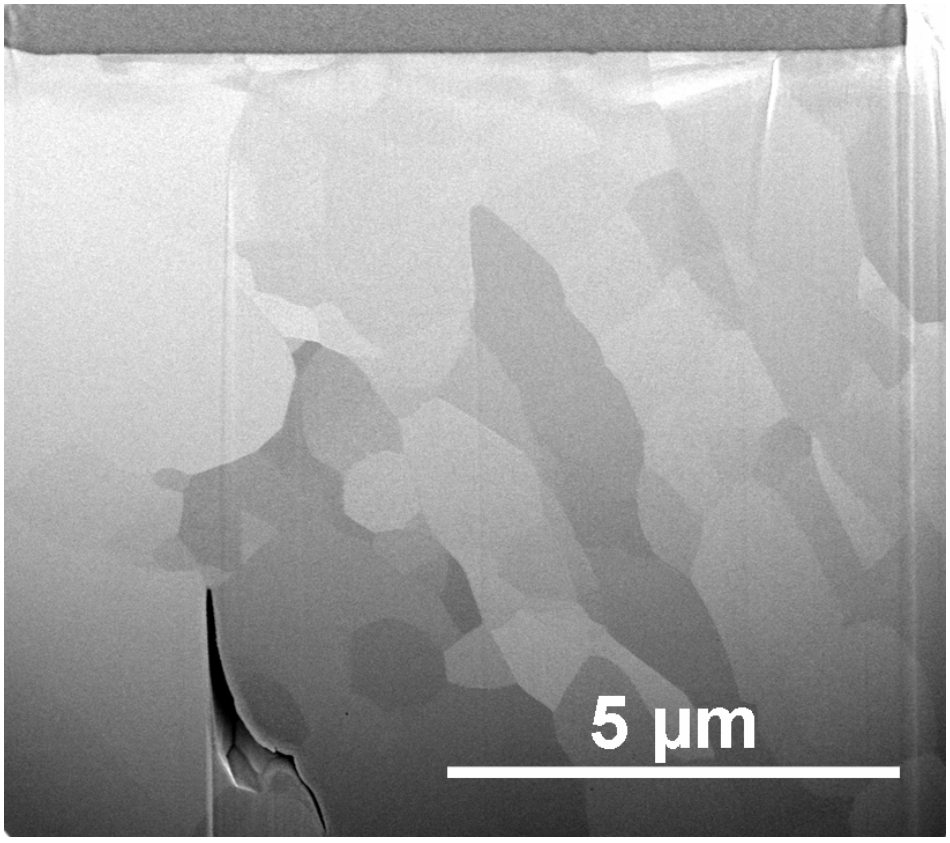

Figure 1. SEM/FIB cross section image of polycrystalline ITER-grade W (tilted by 38°).

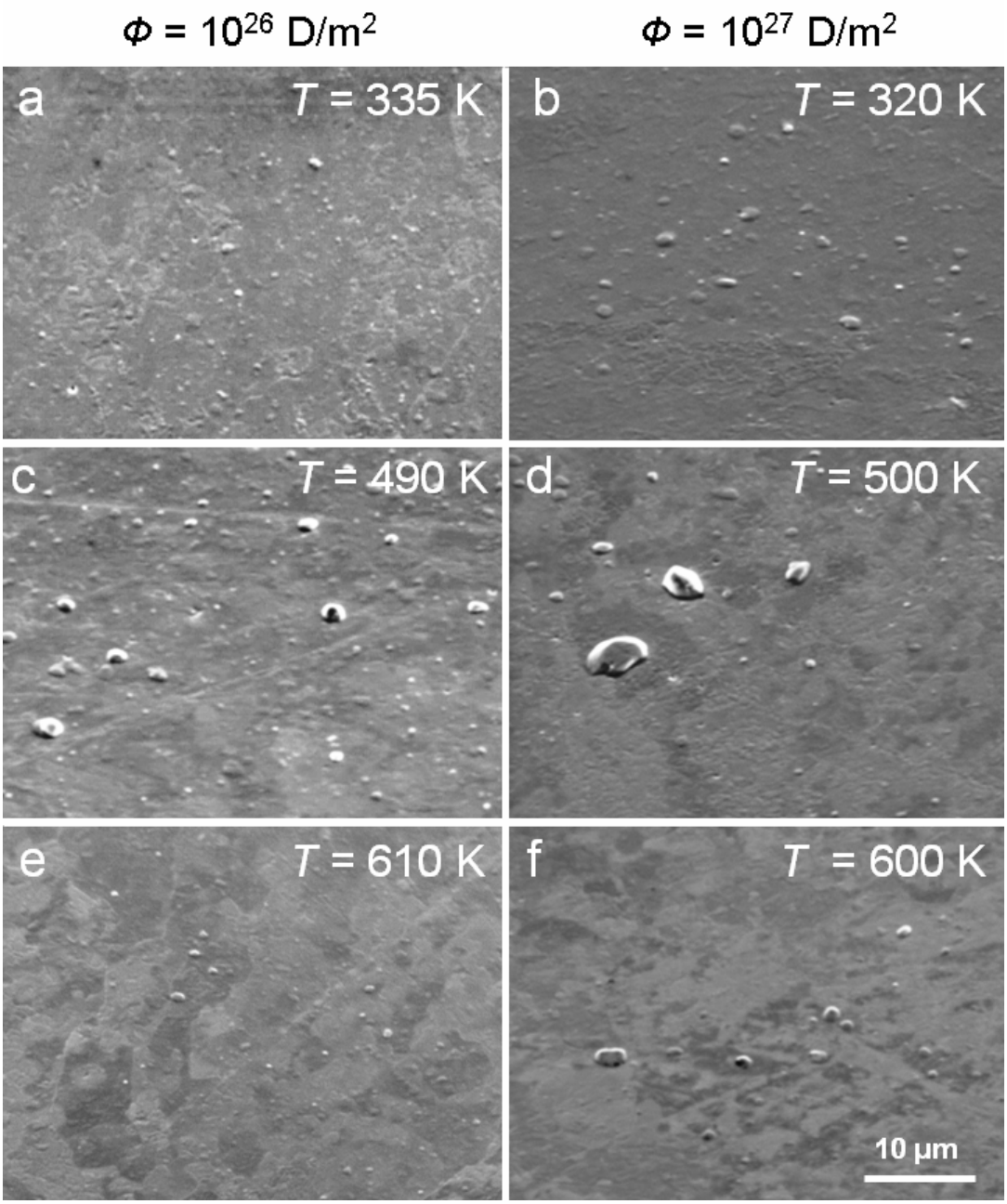

Figure 2. SEM images of polycrystalline ITER-grade W exposed to low-energy (38 eV/D), high-flux (10^{22} D/m^2 s) D plasma with ion fluences, Φ, of 10^{26} D/m^2 (a, c, e – left part of the figure) and 10^{27} D/m^2 (b, d, f – right part of the figure) at indicated temperatures. The scale bar given in panel (f) is valid for all images. The surfaces were tilted at an angle of 45° to the electron beam.

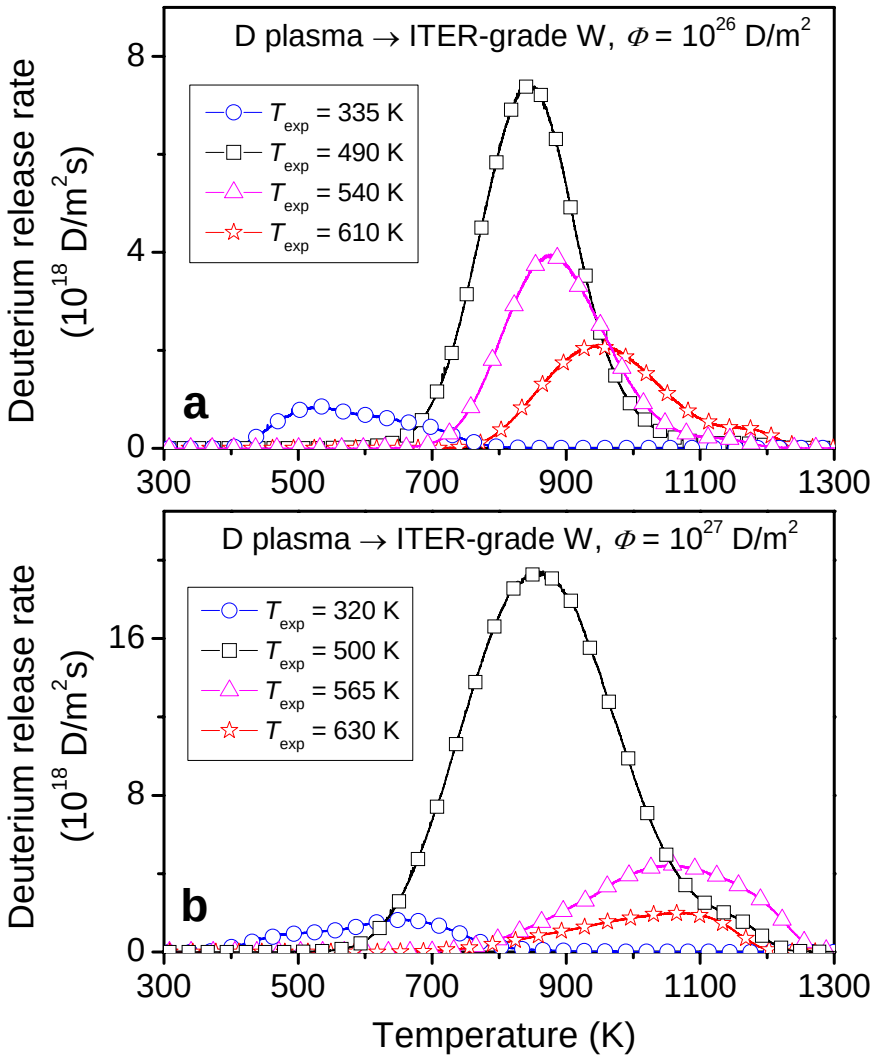

Figure 3. Thermal desorption spectra of deuterium released from polycrystalline ITER-grade W exposed to low-energy (38 eV/D), high-flux (10^{22} D/m^2 s) D plasma with ion fluences of 10^{26} (a) and 10^{27} D/m^2 (b) at various temperatures. The TDS heating rate was 0.5 K/s. Note that the deuterium release rate scales in panels (a) and (b) differ by a factor of 2.5.

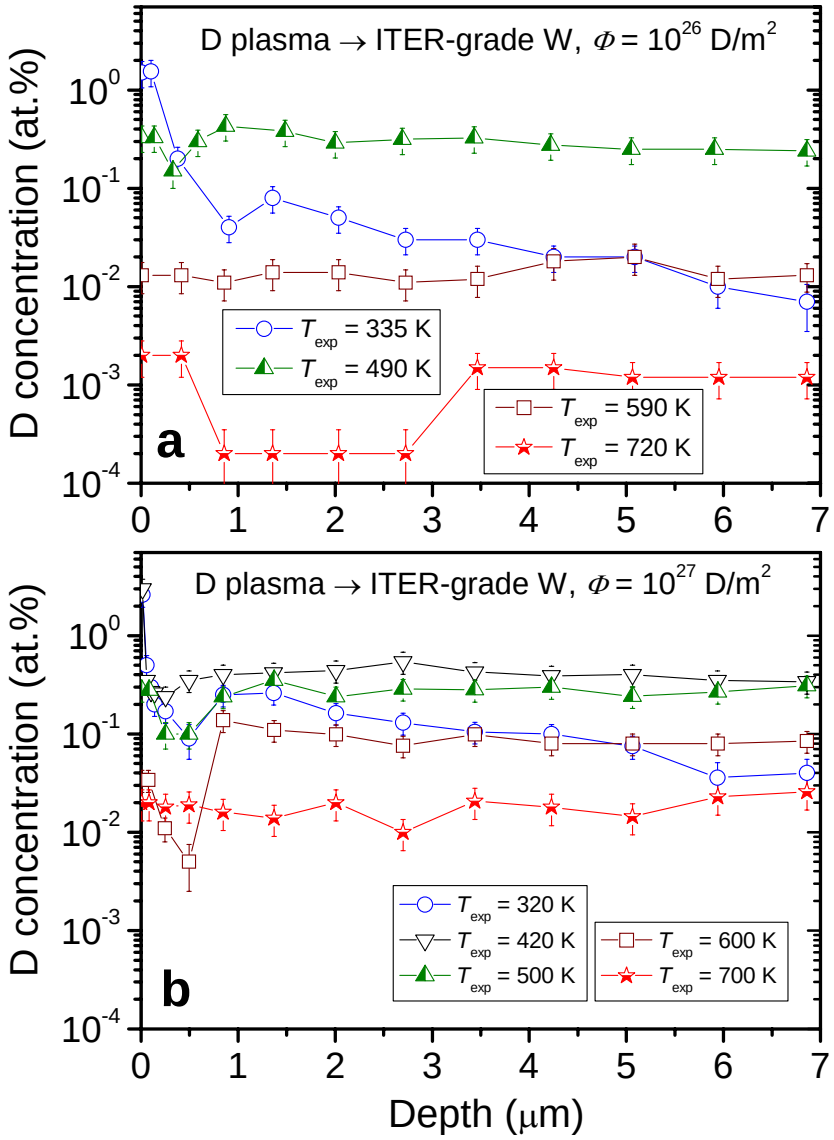

Figure 4. Depth profiles of deuterium retained in polycrystalline ITER-grade W exposed to low-energy (38 eV/D), high-flux (10^{22} D/m^2 s) D plasma with ion fluences of 10^{26} (a) and 10^{27} D/m^2 (b) at various temperatures.

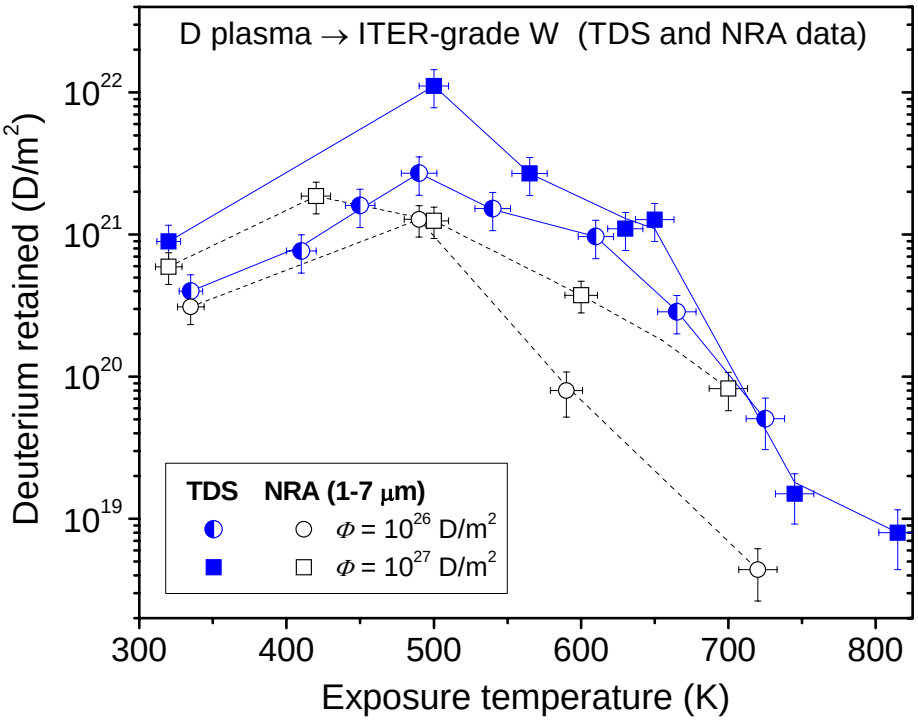

Figure 5. Deuterium retention in polycrystalline ITER-grade W exposed to low-energy (38 eV/D), high-flux (10^{22} D/m^2 s) D plasma with ion fluences of 10^{26} and 10^{27} D/m^2, as a function of the exposure temperature. The total deuterium retention was determined by thermal desorption spectrometry (TDS) (filled symbols), whereas the D retention up to a depth of 7 μm was measured by nuclear reaction analysis (NRA) (open symbols).

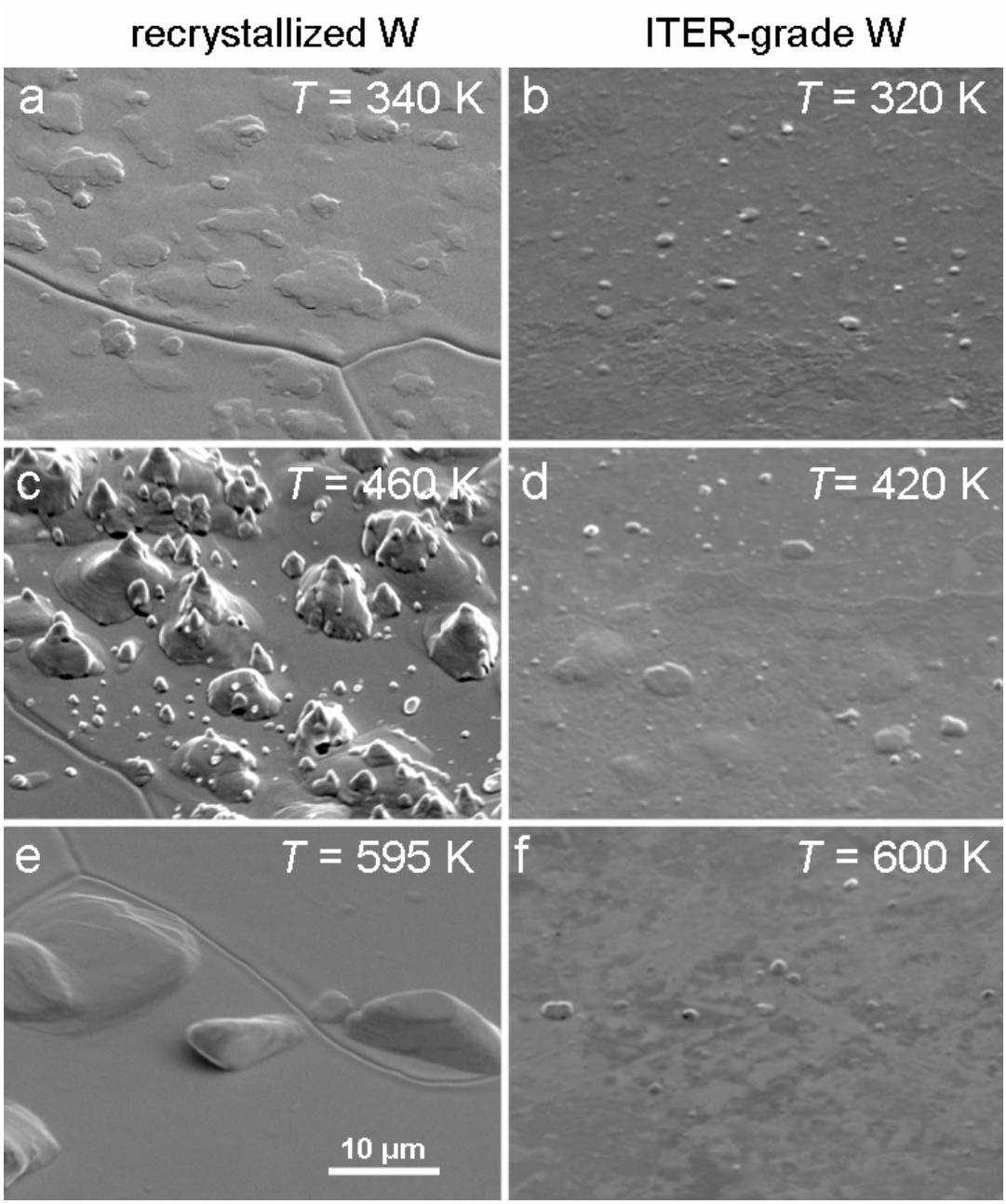

Figure 6. SEM images of recrystallized W (rc-W) (a, c, e – left part of the figure) [9, 15] and polycrystalline ITER-grade W (ITER-W) (b, d, f – right part of the figure) exposed to low-energy (38 eV/D), high-flux (10^{22} D/m^2 s) D plasma with an ion fluence of 10^{27} D/m^2 at indicated temperatures. The scale bar given in panel (e) is valid for all images. The surfaces were tilted at an angle of 45° to the electron beam.

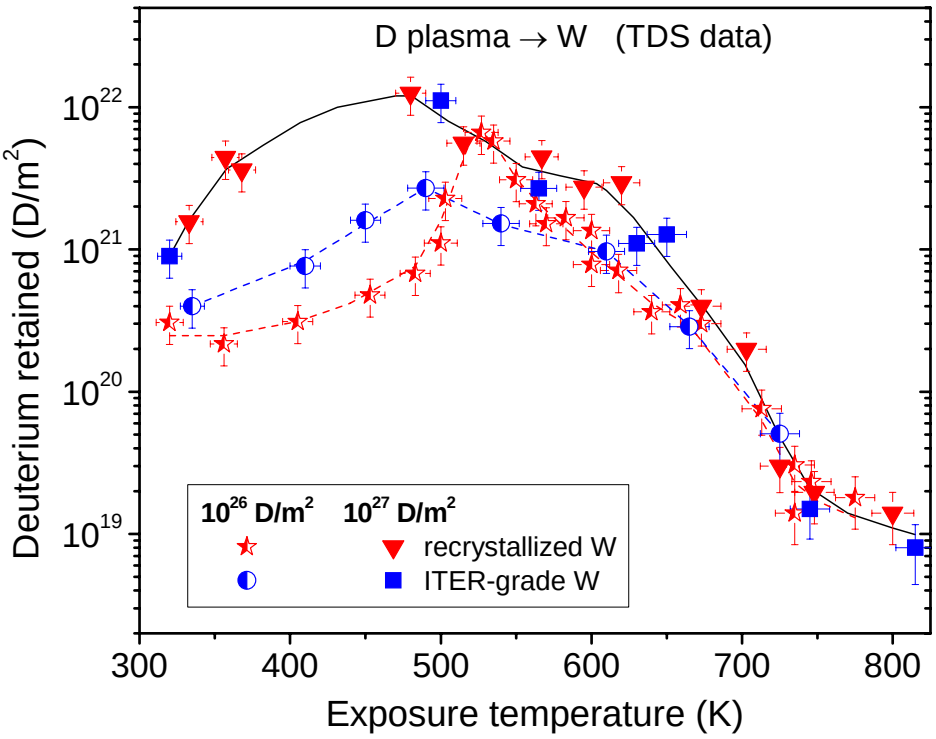

Figure 7. Total deuterium retention in recrystallized W [9, 15] and polycrystalline ITER-grade W exposed to low-energy (38 eV/D), high flux (10^{22} D/m^2 s) D plasma with ion fluences of 10^{26} and 10^{27} D/m^2, as a function of the exposure temperature. The total deuterium retention was determined by thermal desorption spectrometry.

References

[1] G. Federici, P. Andrew, P. Barabaschi, J. Brooks, R. Doerner, A. Geier, A. Herrmann, G. Janeschitz, K. Krieger, A. Kukushkin, A. Loarte, R. Neu, G. Saibene, M. Shimada, G. Strohmayer, M. Sugihara, J. Nucl. Mater. 313-316 (2003) 11.

[2]K. Tobita, S. Nishio, M. Enoeda, M. Sato, T. Isono, S. Sakurai, H. Nakamura, S.Sato, S. Suzuki, M. Ando, K. Ezato, T. Hayashi, T. Hayashi, T. Hirose , T. Inoue, Y. Kawamura, N. Koizumi, Y. Kudo, R. Kurihara, T. Kuroda, M. Matsukawa, K. Mouri, Y. Nakamura, M. Nishi, Y. Nomoto, J. Ohmori, N. Oyama, K. Sakamoto, T. Suzuki, M. Takechi, H. Tanigawa, K. Tsuchiya, D. Tsuru, Fusion Eng. Des. 81 (2006) 1151.

[3] C.H. Skinner, A.A. Haasz, V.Kh. Alimov, N. Bekris, R.A. Causey, R.E.H. Clark, J.P. Coad, J.W. Davis, R.P. Doerner, M. Mayer, A. Pisarev, J. Roth, T. Tanabe, Fusion Sci. Technol. 54 (2008) 891.

[4] A.A. Haasz, M. Poon, J. Davis, J. Nucl. Mater. 266-269 (1999) 520.

[5] K. Tokunaga, M.J. Baldwin, R.P. Doerner, N. Noda, Y. Kubota, N. Yoshida, T. Sogabe, T. Kato, B. Schedler, J. Nucl. Mater. 337-339 (2005) 887.

[6] W.M. Shu, A. Kawasuso, T. Yamanishi, J. Nucl. Mater. 386-388 (2009) 356.

[7] S. Lindig, M. Balden, V.Kh. Alimov, T. Yamanishi, W.M. Shu, J. Roth, Phys. Scr. T138 (2009) 014040.

[8] V.Kh. Alimov, W.M. Shu, J. Roth, K. Sugiyama, S. Lindig, M. Balden, K. Isobe, T. Yamanishi, Phys. Scr. T138 (2009) 014048.

[9] V.Kh. Alimov, W.M. Shu, J. Roth, S. Lindig, M. Balden, K. Isobe, T. Yamanishi, J. Nucl. Mater. (2011), doi: 10.1016/j.jnuclmat.2011.01.088.

[10] G. Kalinin, V. Barabash, S. Fabritsiev, H. Kawamura, I. Mazul, M. Ulrickson, C. Wu, S. Zinkle, Fusion Eng. Des. 55 (2001) 231.

[11] T. Hirai, G. Pintsuk, J. Linke, M. Batilliot, J. Nucl. Mater. 390-391 (2009) 751.

[12] G.-N. Luo, W.M. Shu, H. Nakamura, S. O'Hira, M. Nishi, Rev. Sci. Instrum. 75 (2004) 4374.

[13] V.Kh. Alimov, M. Mayer, J. Roth, Nucl. Instr. and Meth. B 234 (2005) 169.

[14] P. Franzen, B.M.U. Scherzer, W. Möller, Nucl. Instr. and Meth. B 67 (1992) 536.

[15] V.Kh. Alimov, S. Lindig, M. Balden, K. Isobe, W.M. Shu, J. Roth, T. Yamanishi, Annual Report of Hydrogen Isotope Research Center, University of Toyama, Japan, 29 & 30 (2010) 71.

[16] M. Balden, S. Lindig, A. Manhard, J.-H. You, J. Nucl. Mater. 414 (2011) 69.

[17] A. Manhard, U. von Toussaint, T. Dürbeck, K. Schmid, W. Jacob, Phys. Scr. (Proc. 13th Intern. Workshop on Plasma-Facing Materials and Components for Fusion Application, May 9-13, 2011, Rosenheim, Germany).

[18] J.B. Condon and T. Schober, J. Nucl. Mater. 207 (1993) 1.

[19] V.Kh. Alimov, J. Roth, M. Mayer, J. Nucl. Mater. 337-339 (2005) 619.

[20] P. Gumbsch, J. Nucl. Mater. 323 (2003) 304.

[21] S. Lindig, M. Balden, V.Kh. Alimov, A. Manhard, C. Höschen, T. Höschen, B. Tyburska-Püschel, J. Roth, Phys. Scr. (Proc. 13th Intern. Workshop on Plasma-Facing Materials and Components for Fusion Application, May 9-13, 2011, Rosenheim, Germany).